IOP Publishing Journal of Physics: Condensed Matter

J. Phys.: Condens. Matter **21** (2009) 464109 (6pp) doi:10.1088/0953-8984/21/46/464109

Solid–liquid interfacial energies and equilibrium shapes of nanocrystals

R Backofen and A Voigt

Institut für Wissenschaftliches Rechnen, TU Dresdem, 01062 Dresden, Germany

E-mail: rainer.backofen@tu-dresden.de

Received 22 April 2009
Published 27 October 2009
Online at stacks.iop.org/JPhysCM/21/464109

Abstract

We extract the anisotropy of the solid–liquid interfacial energy of small crystals using phase field crystal simulations. The results indicate a strong dependence of the interfacial energy on the parameters in the phase field crystal model determining the position in the solid–liquid coexistence region in the phase diagram. Furthermore a size dependence of the anisotropy is shown if the crystal shape is reduced to the size of a nucleus.

(Some figures in this article are in colour only in the electronic version)

1. Introduction

The solid–liquid interfacial energy γ is one of the fundamental material properties required in mesoscopic models to describe growth morphologies resulting from crystal growth from the melt. Especially if smaller and smaller length scales become of interest, the importance of the interface is increased compared with phenomena in the bulk phases. Such interfaces play a key role in many practically important physical processes, like homogeneous and heterogeneous nucleation, crystal growth, dendritic solidification, surface roughening, thermal faceting and self-organization of nanostructures. Thus a quantitative knowledge of γ is necessary in order to model these processes not only qualitatively. Due to significant challenges associated with direct experimental measurements, various methods have been proposed for computing γ using molecular dynamics; see e.g. [1] for the capillary fluctuation method. Here a quasi-one-dimensional interface is analysed for various orientations and then used to fit an analytic formula describing the orientation dependence of γ. The method has been applied to compute solid–liquid interfacial energies for various materials and the energies obtained are already used in mesoscopic models, e.g. for dendritic solidification [2]. However, the method is costly and only applicable for smooth energies, which rules out functions with cusps. Cusps in the interfacial energy correspond to facets in the interface, which is a common feature for many materials. We propose an approach for extracting γ using classical density functional theory of freezing. Approximations of a dynamic version of the theory, so called phase field crystal models, allow efficient atomic simulations on diffusive timescales, which can be used to compute equilibrium shapes from which γ can be reconstructed.

The outline of the paper is as follows. We first introduce the phase field crystal model and describe a numerical approach for solving the equation efficiently. The algorithm is used to compute equilibrium crystal shapes for various points in the solid–liquid coexistence region of the phase diagram. The density profile and the diffuse interface between the crystal and liquid is analysed and the extracted equilibrium shape used to fit an analytic formula for γ. The last investigation concerns the size dependence of γ if the crystal size reaches a nanometre length scale.

2. Phase field crystal modelling

The phase field crystal model is now widely used in order to predict crystal nucleation and growth on atomic length scales. The PFC model was first developed in [3] and then subsequently applied to many scenarios like interfaces [4], polycrystalline pattern formation [5, 6], commensurate–incommensurate transitions [7], edge dislocations [8], grain boundary pre-melting [9] and colloidal solidification [10]. The model resolves the atomic scale density wave structure of a polycrystalline material and describes the defect-mediated evolution of this structure on timescales orders of magnitude larger than those of molecular dynamic simulations. In its simplest form the phase field crystal model results from the energy

$$F[\psi] = \int_\Omega -|\nabla\psi|^2 + \tfrac{1}{2}(\Delta\psi)^2 + f(\psi)\,\mathrm{d}x$$

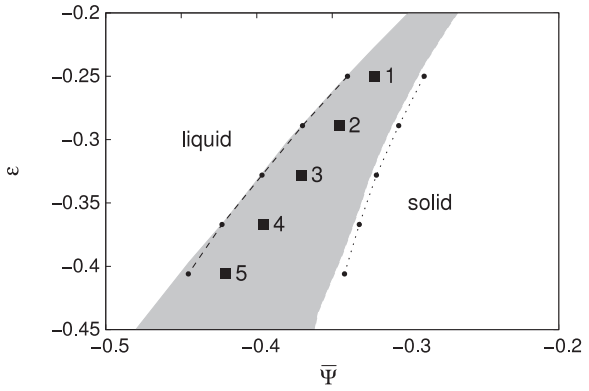

Figure 1. Computed phase diagram of the phase field crystal model. The shaded region is the coexistence region calculated using the one-mode approximation [3]. Big points (1)–(5) correspond to the parameters used in the simulations (1): $(\epsilon; \bar{\psi}) = (-0.25; -0.322)$, (2): $(-0.289; -0.345)$, (3): $(-0.328; -0.370)$, (4): $(-0.367; -0.395)$, (5): $(-0.406; -0.420)$. The small points are $\bar{\psi}$ in the ordered and homogeneous phase.

with $f(\psi) = \frac{1}{2}(1-\epsilon)\psi^2 + \frac{1}{4}\psi^4$, ψ the number density and ϵ a parameter determining the approximation of the liquid structure factor [3]. Comparing the energy with a classical phase field type energy, e.g. $\int_\Omega \frac{\delta}{2}|\nabla\phi|^2 + \frac{1}{\delta}g(\phi)\,\mathrm{d}x$ for an order parameter ϕ, with δ a length scale determining the width of a diffuse interface and $g(\phi)$ a double-well potential, the difference is in the sign of the gradient term and the additional higher order term. The negative sign in the gradient term favours changes in ψ, whereas the higher order term favours suppression of such changes. The competition between the two terms introduces a fixed length scale for which the energy will be minimized. This length scale is used to model the periodicity of a crystal lattice. The formulation used here favours a bcc ordering in three dimensions and a hexagonal close packed structure in two dimensions. The dynamic laws constructed to minimize the free energy are the non-conserved Swift–Hohenberg equation (L^2-gradient flow)

$$\partial_t \psi = -\frac{\delta F[\psi]}{\delta \psi}$$

and the conserved phase field crystal model (H^{-1}-gradient flow)

$$\partial_t \psi = \nabla \cdot \left(\nabla \frac{\delta F[\psi]}{\delta \psi} \right),$$

with the variational derivative given by

$$\frac{\delta F[\psi]}{\delta \psi} = \Delta^2 \psi + 2\Delta\psi + f'(\psi).$$

Although this formulation is phenomenological, the model can be derived starting from a Smoluchowski equation via dynamic density functional theory using various approximations [11, 12, 10] and thus provides also a quantitative atomic theory which operates on diffusive timescales.

This leads to a non-constant mobility $(\psi + 1)$ in the phase field crystal model

$$\partial_t \psi = \nabla \cdot ((\psi + 1)\nabla(\Delta^2 \psi + 2\Delta\psi + f'(\psi)))$$

and we write the non-linear sixth-order equation as a system of three second-order equations

$$\partial_t \psi = \nabla \cdot ((\psi + 1)\nabla u)$$

$$u = \Delta v + 2\Delta\psi + f'(\psi)$$

$$v = \Delta\psi$$

for which a stable semi-implicit finite element discretization is introduced in [12]. We use this approach but with higher order elements and an adaptive time-stepping strategy, which allows us to use large time steps if the system is close to equilibrium. The algorithm is implemented in the adaptive finite element toolbox AMDiS [13].

3. Using the phase field crystal model to compute equilibrium shapes

In [5] the phase field crystal model is used to reproduce the magnitude and anisotropy of the interfacial free energy of Fe using amplitude equations following from a small ϵ analysis of the phase field crystal equation. Molecular dynamic simulations with an inter-atomic potential for Fe are used to compute the free parameters in the phase field crystal model. The results obtained are in nice agreement with previous molecular dynamic calculations for the interfacial energy. In [14] a similar approach is used, in which the amplitude equations are constructed directly from density functional theory not using the approximations made in the phase field crystal model.

We will here not focus on a specific material but describe a general approach for computing equilibrium shapes using the phase field crystal model from which we reconstruct γ. Furthermore we determine the dependence of the anisotropy in the interfacial free energy on the parameter ϵ. ϵ and the average density $\bar{\psi}$ are the only remaining free parameters in the phase field crystal energy and determine the position in the phase diagram, which can be computed using a one-mode approximation; see figure 1.

All parameter sets are within the coexistence region of liquid and solid, which allows us to eliminate kinetic effects in the computation of the equilibrium shapes. Also the mobility can be set to a constant, as we are only interested in equilibrium states. We will use a two-dimensional setting in which an initial island is nucleated in the centre of the liquid and grows until it reaches its equilibrium. We therefore start with a homogeneous liquid phase with initial fluctuations. The fluctuation is chosen with respect to the lattice structure of the expected crystal. All boundaries are set to no flux conditions. Detailed simulations have been performed to eliminate the effects of the computational domain and the underlying mesh on the equilibrium shape. Due to the symmetry only 1/12 of the domain is computed and only 1/4 of the computed equilibrium crystal is shown in figure 2, ranging from a circular shape for parameter set (1) to a fully hexagonal shape for parameter set (5).

For a more quantitative analysis of the equilibrium we need to reconstruct the shape from the density profile. But due

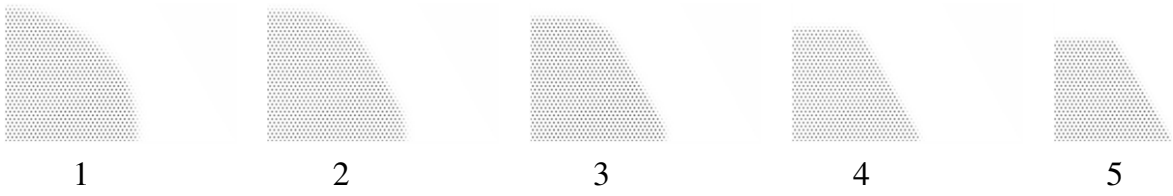

Figure 2. Computed density fields for equilibrium shape for parameter sets (1)–(5) using a constant mobility.

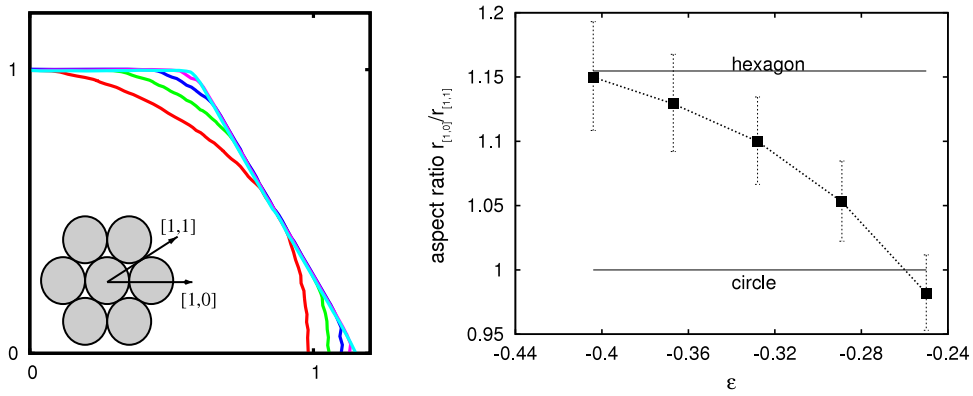

Figure 3. Left: extracted envelope of the equilibrium shapes in figure 2. The envelopes are normed to the same radial distance of the facet. Right: computed aspect ratio of the radial distance for $\theta = 0$ ([10] orientation) and $\theta = \frac{\pi}{6}$ ([11] orientation), with error bars resulting from the uncertainty in determining the equilibrium shape.

to the atomic nature of the crystal structure and the gradual transition between the crystal and the homogeneous liquid, the shape of the crystal has to be defined with care.

We construct an indicator function for the crystal using the value of the density at the position defined by the ideal crystal structure which leads to a maximum value in the crystalline phase and a minimal value in the liquid. Thus the envelope is defined as the region where the indicator function varies. Due to the periodicity of the crystal the crystal size does not vary continuously within our construction. It thus contains an uncertainty of the order of one lattice spacing, which determines the error bars for all quantities that we extract from the computed crystal shape. Figure 3 shows the envelope of the computed shapes.

The extracted crystal shape shows a fully faceted structure with sharp corners for the parameter set (5), corresponding to the lowest temperature. With increasing temperature for parameter sets (4)–(2) the facets remain; however the corners become rounded with an increasing radius. For parameter set (1), corresponding to the highest temperature, the radius of the rounded corner is large enough to let the facet disappear and the resulting shape is circular.

4. The transition zone and the decay of density waves in liquid

We now turn to analysing the transition zone, between solid and liquid. The phase field crystal model determines a diffuse interface between solid and liquid, which has been used to construct classical phase field models for an order parameters ϕ from the phase field crystal model. The diffuse interface width corresponds to the parameter δ in the classical phase field energy introduced above. Our simulations however indicate that the diffuse interface width strongly depends on the parameter set used; see figure 4.

For parameters set (5), corresponding to the lowest temperature, the transition zone is narrow and with increasing temperature, parameter sets (4)–(1), the transition zone becomes wider. Furthermore also the rate of decay of the density waves in the liquid depends on the parameter set. The waves decay fastest for parameter set (5) and slowest for parameter set (1). The number density profiles obtained are very similar to profiles computed using molecular dynamics [15, 16].

5. Solid–liquid interfacial energy

Given the solid–liquid interfacial energy γ the equilibrium shape of the crystal can be constructed. The shape is defined as the shape of minimum interfacial energy under the constraint of fixed area [17]. The interfacial energy $\gamma = \gamma(\theta)$ depends on the local orientation θ of the interface normal, reflecting the anisotropy of the material. According to the Wulff theorem [18], the equilibrium shape may be constructed as follows: draw at each point of the polar plot of $\gamma(\theta)$ a straight line perpendicular to the normal direction; the inner envelope of the resulting family of lines is geometrically similar to the equilibrium shape. Depending on the details of γ the equilibrium shape may contain facets and corners. Facets occur when γ has cusps and corners occur if the stiffness $\tilde{\gamma} = \gamma(\theta) + \gamma''(\theta)$ becomes negative for some orientations. In the latter case it is energetically favourable to exclude high energy

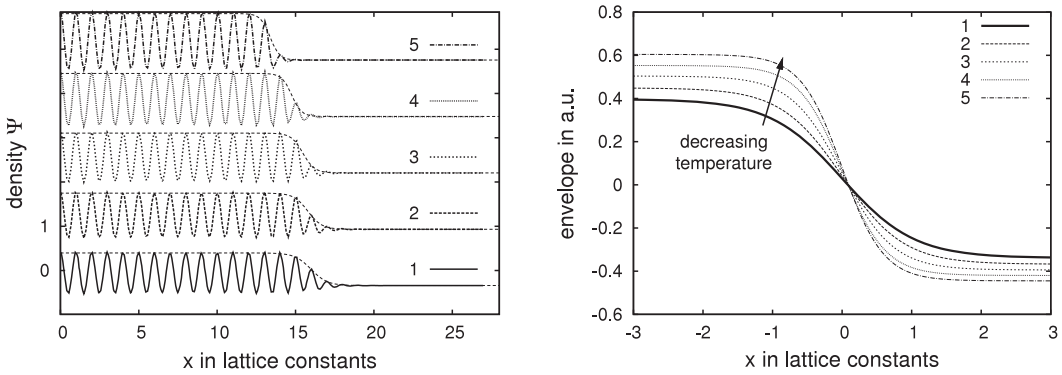

Figure 4. Density profile (left) and transition zone (right) in the direction of the corner ($\theta = 0$ of [10] orientation) for parameter sets (1)–(5). The envelope is only defined at the lattice (density peak) positions. In between, the envelope is defined by fitting a appropriate tanh profile.

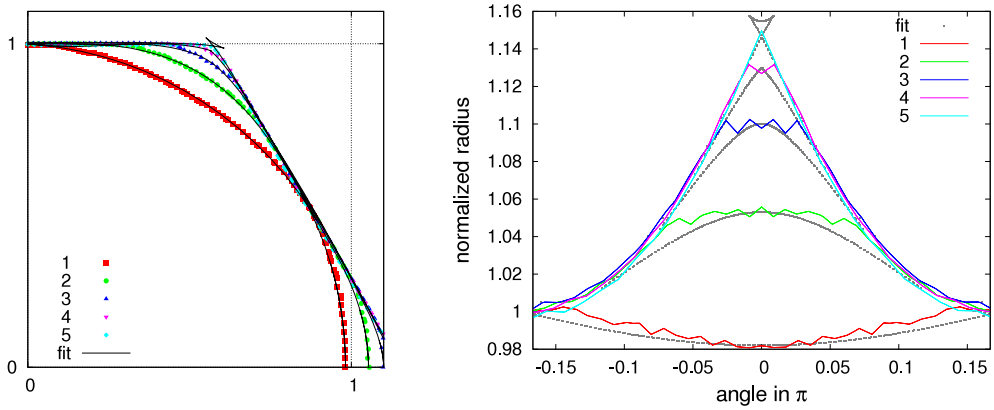

Figure 5. Comparison of computed equilibrium shape and Wulff plot for parameter sets (1)–(5). Left: polar plot; right: detailed plot of the normalized radius over the angle. The values for α are: (1) 0.02, (2) 0.05, (3) 0.10, (4) 0.13 and (5) 0.18.

orientations, i.e. the Wulff shape has missing orientations. For $T = 0$ the equilibrium shape of crystals is assumed to be faceted, which can be understood from simple lattice models. As the temperature increases, these facets shrink and finally disappear at the roughening temperature. As we only consider two-dimensional systems, the interface is a one-dimensional object and the roughening temperature should be zero in these models. So at least for short range interactions the equilibrium shape for $T > 0$ should be smoothly curved. However this is not the case in our simulations. For a detailed discussion of the thermodynamics and statistical mechanics of equilibrium crystal shapes we refer the reader to [19].

Here we are facing the opposite situation. Given an equilibrium shape we would like to compute the solid–liquid interfacial energy γ, which is much less straightforward. In particular, different γ might lead to the same equilibrium shape. We therefore use only a generic function for γ and adjust the parameters in order to reconstruct the computed equilibrium shape, in particular the aspect ratio. The function should be able to allow for cusps. In [20] a generic function is used which adapted to our situation reads

$$\gamma(\theta) = \gamma_0\left(1 + \alpha\left|\cos\left(\frac{n\theta}{2}\right)\right|\right)$$

with α the strength of the anisotropy and $n = 6$ indicating the sixfold symmetry. As long as $\tilde{\gamma} \geqslant 0$ we obtain for the aspect ratio

$$\frac{\gamma(0)}{\gamma(\frac{\pi}{6})} = 1 + \alpha.$$

We therefore can compute the strength of the anisotropy as $\alpha = \frac{\gamma(0)}{\gamma(\frac{\pi}{6})} - 1 = \frac{r(0)}{r(\frac{\pi}{6})} - 1$ and only have to measure the radial distance r of the extracted equilibrium shape at the two orientations 0 and $\pi/6$. Using the Wulff construction for γ with the parameters obtained for α, we get the Wulff shape. Figure 5 shows a comparison of the equilibrium shapes computed using the phase field crystal method and the Wulff shape.

Excellent agreement is achieved in the polar plot. Differences are only visible in the detailed plot on the right which indicates that our chosen free energy γ underestimates the length of the facets and smooths the corners not with a circular arc. However, due to the uncertainty in the reconstruction of the equilibrium shape from the density profile we will not further analyse these differences, as they are smaller than the error bars mentioned above.

Using the analogy of the one-dimensional interface with a step on a vicinal surface, we can also compare our results with a step energy. In [21] a low temperature formula for the step energy on a (111) surface with next neighbour interaction is derived from a lattice gas on a hexagonal grid. An analytic

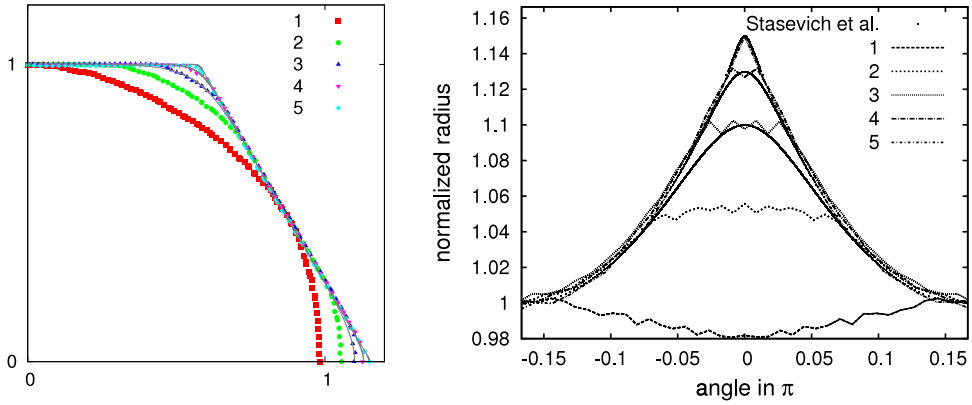

Figure 6. Comparison of equilibrium shapes computed using the low temperature expansion of Stasevich *et al* [21] and the Wulff plot for parameter sets (3)–(5). Left: polar plot; right: detailed plot of the normalized radius over the angle.

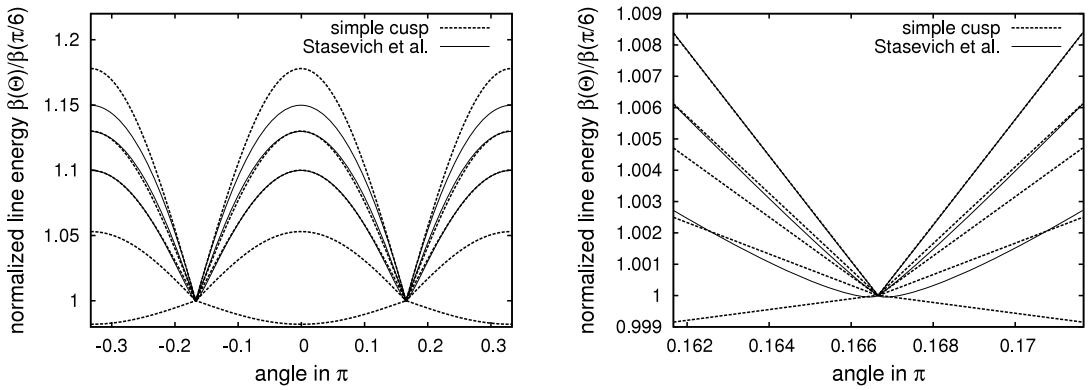

Figure 7. The line energy of the simple cusp model and the model of Stasevich *et al* [21] are compared. The maxima of the line energy decrease with increasing ϵ. That is, the plot with the highest maximum corresponds to simulation (5).

formula valid for low temperatures and all orientation is obtained, which reads

$$\beta(\Theta) = \beta_0\left[\eta_+(\Theta) - \frac{t}{\ln(3)}(s_+(\Theta) - s_-(\Theta) - s_0(\Theta))\right]$$

and is specified in terms of normalized temperature $t = \frac{T}{T_c} = \frac{k_B T \ln(3)}{2\epsilon}$ with $\beta_0 = \frac{2\epsilon}{a}$. ϵ the bonding energy, T_c the critical temperature and a the distance of next nearest neighbours. s_i and η_i are defined through $\eta_\pm(\Theta) = \cos(\Theta) \pm \frac{\sin(\Theta)}{\sqrt{3}}$, $\eta_0(\Theta) = \frac{2}{\sqrt{3}}\sin(\Theta)$, $s_i(\Theta) = \eta_i(\Theta)\ln(\eta_i(\Theta))$ for $i = +, 0, -$.

Figure 6 shows the comparison of this formula with the data extracted from the PFC simulation. As indicated in [21] the low temperature expansion is only valid to about $T = T_c/8$ which corresponds to our parameter sets (3)–(5). We again obtain an excellent agreement within the possible accuracy.

Finally we compare the two models in figure 7. As long as the stiffness is positive, the two models are very similar. Only for a very large anisotropy do the models differ, because the simple cusp model produces 'ears' in the Wulff shape.

6. Size dependence of the equilibrium shapes and interfacial energy

The solid–liquid interfacial energy is a microscopic quantity assuming a continuous interface. In order to reach this limit the computational domain and the crystal size have been chosen as large as possible to eliminate atomic effects. Our goal now is to reduce the size of the crystal to find the smallest possible stable equilibrium shape. We therefore start with the equilibrium configuration discussed above and reduce mass in the liquid phase. The relaxation of the system results in melting of the crystal and the formation of a smaller equilibrium crystal. An iterative process leads to the smallest possible crystal, which is characterized by the fact that a further reduction of mass in the system will lead to a homogeneous liquid phase. It is assumed that the minimal crystal obtained is related to the nuclei in homogeneous nucleation. However, our minimal crystal is defined in the coexistence region of solid and liquid, whereas the nuclei are typically defined in an undercooled liquid. We observe a change in the shape of the crystal. Figure 8 shows the obtained equilibrium shapes starting from the parameter set (1), the circular shape for the large crystal.

The smaller the crystal gets, the more faceted the equilibrium becomes. The strength of the anisotropy thus becomes a function of the crystal size. A size dependence of the solid–liquid interfacial energy has been discussed in [22]. Here however only the magnitude of the solid–liquid interfacial energy γ_0 is considered and not its dependence on the orientation. Analytical approaches indicate that γ_0 should be related to the surface/volume ratio with a $1/r$ relationship. Thus γ_0 increases for decreasing r, which is specified for

Figure 8. Size dependence of the equilibrium shape starting from parameter set (1).

various materials. Combined with our results, this gives an indication of a strong relation between crystal size and solid–liquid interfacial energy γ on a nanometre length scale.

Using continuum models on the nanoscale thus should be considered with care and might require us to account for such size dependence of the interfacial energy.

7. Conclusion

We have used the phase field crystal model to compute equilibrium crystal shapes in a solid–liquid coexistence regime. Techniques are described for extracting the equilibrium shape from the density profile. An analytic form for the solid–liquid interfacial energy γ, allowing for cusps, is used to fit the equilibrium shapes using the Wulff construction. With this approach we compute γ for various points in the phase diagram ranging from constant functions, leading to a circular crystal shape, to a cusped function, which leads to a fully faceted hexagonal crystal shape. Detailed analysis of the density field also indicates a dependence of the width of the transition zone between crystal and liquid and the decay of the density waves in the liquid on the position in the phase diagram. First results on a dependence of the width of the transition zone on orientation also indicate a sharpening towards the facet, which is in agreement with the behaviour of classical anisotropic phase field models (see [23]), but does not support new concepts for dealing with anisotropic energies in phase field models, as introduced in [24]. A detailed analysis of the angular dependence of the transition zone will be discussed in a forthcoming paper.

Acknowledgments

We would like to thank K Elder for valuable discussions. RB and AV acknowledge support from the DFG via Vo899/7-1 within SPP 1296.

References

[1] Hoyt J J, Asta M and Karma A 2001 Method for computing the anisotropy of the solid–liquid interfacial free energy *Phys. Rev. Lett.* **86** 5530–3

[2] Hoyt J J, Asta M, Haxhimali T, Karma A, Napolitano R E, Trivedi R, Laird B B and Morris J R 2004 Crystal–melt interfaces and solidification morphologies in metals and alloys *MRS Bull.* **29** 935–9

[3] Elder K R, Katakowski M, Haataja M and Grant M 2002 Modeling elasticity in crystal growth *Phys. Rev. Lett.* **88** 245701

[4] Athreya B P, Goldenfeld N, Danzig J A, Greenwood M and Provatas N 2007 Adaptive mesh computation of polycrystalline pattern formation using a renormalization-group reduction of the phase-field crystal model *Phys. Rev.* E **76** 056706

[5] Wu K-A and Karma A 2007 Phase-field crystal modeling of equilibrium bcc–liquid interfaces *Phys. Rev.* B **76** 184107

[6] Goldenfeld N, Athrya B P and Dantzig J A 2005 Renormalization group approach to multiscale simulation of polycrystalline materials using the phase-field crystal model *Phys. Rev.* E **72** 020601

[7] Achim C V, Karttunen M, Elder K R, Ala-Nissilä T and Ying S C 2006 Phase diagram and commensurate–incommensurate transitions in the phase-field crystal model with an external pinning potential *Phys. Rev.* E **74** 021104

[8] Berry J, Grant M and Elder K R 2006 Diffuse atomic dynamics of edge dislocations in two dimensions *Phys. Rev.* E **73** 031609

[9] Mellenthin J, Karma A and Plapp M 2008 Phase-field crystal study of grain-boundary premelting *Phys. Rev.* B **78** 184110

[10] van Teeffelen S, Backofen R, Voigt A and Löwen H 2009 Derivation of the phase field crystal model for colloidal solidification *Phys. Rev.* E **79** 051404

[11] Elder K R, Provatas N, Berry J, Stefanovic P and Grant M 2007 Phase-field crystal modeling and classical density functional theory of freezing *Phys. Rev.* B **75** 064107

[12] Backofen R, Rätz A and Voigt A 2007 Nucleation and growth by a phase-field crystal (PFC) model *Phil. Mag. Lett.* **87** 813–20

[13] Vey S and Voigt A 2007 AMDiS—adaptive multidimensional simulations *Comput. Vis. Sci.* **10** 57–66

[14] Majaniemi S and Provatas N 2009 Deriving surface-energy anisotropy for phenomenological phase-field models of solidification *Phys. Rev.* E **79** 011608

[15] Davischack R L and Laird B B 1998 Simulation of the hard-sphere crystal–melt interface *J. Chem. Phys.* **108** 9452–62

[16] Sun D Y, Asta M and Hoyt J J 2004 Crystal–melt interfacial free energies and mobilities in fcc and bcc Fe *Phys. Rev.* B **69** 174103

[17] Herring C 1963 *Structure and Properties of Solid Surfaces* (Chicago, IL: University of Chicago Press) pp 5–81

[18] Wulff G 1901 Zur Frage der Geschwindigkeit des Wachstums und der Auflösung der Kristallflächen *Z. Kristallogr.* **34** 449–530

[19] Rottman C and Wortis M 1984 Statistical mechanics of equilibrium crystal shapes: interfacial phase diagrams and phase transitions *Phys. Rep.* **103** 59–79

[20] Bonzel H P and Preuss E 1995 Morphology of periodic surface profiles below the roughening temperature: aspects of continuum theory *Surf. Sci.* **336** 209–24

[21] Stasevich T J, Gebremariam H, Einstein T L, Geissen M, Steiner C and Ibach H 2005 Low-temperature orientation dependence of step stiffness on (111) surfaces *Phys. Rev.* B **71** 245414

[22] Jiang Q and Lu H M 2008 Size dependent interface energy and its applications *Surf. Sci. Rep.* **63** 427–64

[23] Kobayashi R 1993 Modeling sand numerical simulations of dendritic crystal growth *Physica* D **63** 410–23

[24] Torabi S, Lowengrub J, Voigt A and Wise S 2009 A new phase-field model for strongly anisotropic systems *Proc. R. Soc.* A **465** 1337–59